Science of the Total Environment 631–632 (2018) 723–732

Contents lists available at ScienceDirect

Science of the Total Environment

journal homepage: www.elsevier.com/locate/scitotenv

Generating false negatives and false positives for As and Mo concentrations in groundwater due to well installation

Ilka Wallis [a,b], Thomas Pichler [c,d,*]

[a] College of Science and Engineering, Flinders University, GPO Box 2100, Adelaide, SA 5001, Australia
[b] National Centre for Groundwater Research and Training, Adelaide, GPO Box 2100, SA 5001, Australia
[c] Department of Geosciences, University of Bremen, 28334 Bremen, Germany
[d] Department of Earth Sciences, Dartmouth College, Hanover, NH 03755, USA

HIGHLIGHTS

- Well installation triggers redox reactions causing Mo and As release to groundwater.
- As release follows pyrite oxidation.
- Mo is mobilized during organic matter mineralization.
- Leaching experiments and quantification of stoichiometric ratios through modelling
- Natural attenuation within one year within short transport distances

GRAPHICAL ABSTRACT

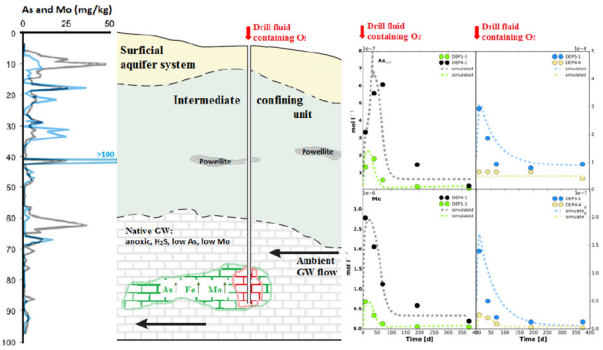

ARTICLE INFO

Article history:
Received 29 January 2018
Received in revised form 21 February 2018
Accepted 6 March 2018
Available online xxxx

Editor: José Virgílio Cruz

Keywords:
Arsenic
Molybdenum
Geogenic contamination
Well installation
Reactive transport modelling

ABSTRACT

Groundwater monitoring relies on the acquisition of 'representative' groundwater samples, which should reflect the ambient water quality at a given location. However, drilling of a monitoring well for sample acquisition has the potential to perturb groundwater conditions to a point that may prove to be detrimental to the monitoring objective. Following installation of 20 monitoring wells in close geographic proximity in central Florida, opposing concentration trends for As and Mo were observed. In the first year after well installation As and Mo concentrations increased in some wells by a factor of 2, while in others As and Mo concentrations decreased by a factor of up to 100. Given this relatively short period of time, a natural change in groundwater composition of such magnitude is not expected, leaving well installation itself as the likely cause for the observed concentration changes. Hence, initial concentrations were identified as 'false negatives' if concentrations increased with time or as 'false positives' if concentrations decreased. False negatives were observed if concentrations were already high, i.e., the As or Mo were present at the time of drilling. False positives were observed if concentrations were relatively lower, i.e., As or Mo were present at low concentrations of approximately 1 to 2 μg/L before drilling, but then released from the aquifer matrix as a result of drilling. Generally, As and Mo were present in the aquifer matrix in either pyrite or organic matter, both of which are susceptible to dissolution if redox conditions change due to the addition of oxygen. Thus, introduction of an oxidant into an anoxic aquifer through use of an oxygen saturated drilling fluid served as the conceptual model for the trends where concentrations decreased with time. Mixing between drilling fluid and groundwater (i.e., dilution) was used as the conceptual model for scenarios where increasing trends were observed. Conceptual models were successfully tested through formulation and application

* Corresponding author at: Department of Geosciences, University of Bremen, 28334 Bremen, Germany.
E-mail address: pichler@uni-bremen.de (T. Pichler).

https://doi.org/10.1016/j.scitotenv.2018.03.063

of data-driven reactive transport models, using the USGS code MODFLOW in conjunction with the reactive multicomponent transport code PHT3D.

1. Introduction

The installation of wells to monitor groundwater is a common and necessary practice to study the release of contaminants from for example landfills and industrial facilities. Their installation involves drilling into various types of geologic formations with varying subsurface conditions that require different drilling methods and installation procedures. Since it is paramount to obtain 'representative' groundwater samples it is necessary to collect samples that are minimally affected by their acquisition. This should be common knowledge, but often the installation of monitoring wells is not adequate for their intended purpose. Nielsen and Schalla (2006) estimated that > 65 % of groundwater monitoring wells installed in North America since the late 1970s were improperly designed for their intended purpose. Additional complication can be added by the actual drilling of the well if water or air are used as drilling fluids (e.g., Ruda and Farrar, 2006), because the use of water has the inherent problem of introducing metals into the aquifer, while the use of air can introduce hydrocarbons released from the compressor (e.g., Bennett et al., 1988). These are well-known problems and have been addressed through the use of various approaches including a variety of tracers (e.g., Richards et al., 2015 and references therein).

Surprisingly, the introduction of oxygen into aquifers, whether in its gaseous or dissolved form, has not found any attention in the context of well drilling. A possible explanation could be that oxygen is generally not considered a detriment to water quality, although mobilization of redox sensitive metals such as Ni, As and Cu as a result of the introduction of oxidants has been recognized as a potential hazard in the context of in-situ chemical oxidation remedial techniques, or air sparging (e.g. Crimi and Siegrist, 2003). Air sparging in the presence of sufficient ferrous iron (Fe^{2+}), may also reduce the concentration of As due to precipitation of ferrihydrite and subsequent adsorption of As (Brunsting and McBean, 2014). There are several occurrences where the introduction of oxygen into a reducing aquifer caused the release of metals and metalloids from the aquifer matrix (e.g., Jones and Pichler, 2007; Lazareva et al., 2015; Wallis et al., 2011). Introduction of oxygen can trigger a shift from reducing to oxidizing conditions, causing the dissolution of redox sensitive phases such as pyrite and organic matter, both of which are known to frequently contain substantial concentrations of potentially toxic elements such as molybdenum (Mo) and arsenic (As) (Price and Pichler, 2006; Tribovillard et al., 2004). Thus, the installation of a monitoring well could lead to elevated concentrations of redox sensitive metals that were not present in groundwater or in the drilling fluid prior to well installation ('false positives'). With time, such elevated concentrations will decrease due to dilution through groundwater flow or geochemical reactions such as sorption or co-precipitation, while returning to pre-installation physicochemical conditions. If not recognized, this would prove detrimental if the monitoring well was intended to monitor natural attenuation of contamination (e.g., Reisinger et al., 2005). On the other hand, if the contaminating element was present in groundwater at the time of well installation then the use of water during drilling would lower its concentration due to dilution ('false negatives'). Therefore, drilling of a monitoring well in the context of naturally occurring redox sensitive metals in the aquifer matrix can lead to two possible observations: (1) relatively lower concentrations ('false negatives') or (2) relatively higher concentrations of a given contaminant ('false positives'). Despite the extensive body of literature on groundwater contamination due to well installation, this problem has presently not found any scientific consideration.

We report on monitoring wells in central Florida, of which most showed initial As and Mo concentrations exactly as theoretically predicted: If concentrations were relatively high monitoring initially produced 'false negatives' and if concentrations were relatively low monitoring produced 'false positives'. To understand the geochemical processes controlling the observed concentration changes we used time series data in combination with coupled flow and process-based reactive transport modelling.

2. Study area

The field site is located in the municipality of Lithia, approximately 30 km southeast of Tampa, Florida, where during a survey of 96 private supply wells, 20 wells had As concentrations above the current drinking water standard of 10 μg/L and 42 wells had Mo concentrations above USEPA recommend threshold of 40 μg/L. Maximum concentrations were 370 μg/L for As and 4740 μg/L for Mo. Lacking an anthropogenic source As and Mo were determined to be of geogenic origin (Pichler and Mozaffari, 2015; Pichler et al., 2017).

To further study and monitor the problem the Florida Department of Environmental Protection (FDEP) installed 20 monitoring wells as five monitoring well clusters (DEP1, -2, -3, -4 and -5) consisting of four wells screened at depths of approximately 44 m, 62 m, 77 m and 90 m below surface (Pichler and Mozaffari, 2015; Pichler et al., 2017). The wells were spatially distributed throughout the area of elevated concentrations (DEP1 to DEP4) and at a background location located outside of the area of known elevated concentrations (DEP5) (for a map please see Fig. 1 in Pichler and Mozaffari, 2015). The well clusters were completed utilizing rotosonic drilling technology with oxygen-saturated surface water from the nearby Alafia river used as drilling fluid. In the study area, the Alafia is mainly fed by groundwater of the Intermediate and upper Floridan aquifer system (Southwest Florida Water Management District, 2001) and thus, its chemical composition except for oxygen is more or less identical to that of the groundwater in the DEP wells. The individual wells were constructed of two-inch inner diameter flush joined, PVC schedule 40 casing with 6 m of 0.010-inch machine slotted screen sections. A filter pack of 20/30 (U.S. Standard Sieve) silica sand was emplaced around and 3 ft above the screened interval of each well. An interval of bentonite chips was then added to isolate the sand interval from the open borehole. The remaining annular space was grouted and the wells were developed by pumping with a submersible pump until the purge water was clear and free of sediment.

2.1. Hydrogeology

The DEP wells were drilled into a multilayered aquifer system of Tertiary age, which underlies the Lithia area. Three distinct hydrostratigraphic units, can be distinguished, which are, from the top down, the Surficial Aquifer System (SAS), the Intermediate Aquifer System (IAS), and the Upper Floridian Aquifer System (UFA). Katz et al. (2007) and Hughes et al. (2009) provided detailed mineralogical and lithologic descriptions of these units and their regional hydrogeology in central Florida. The unconfined SAS consists of unconsolidated to poorly indurated clastic deposits with depths to the water table ranging from about 3 to 15 m below land surface (Katz et al., 2009). The SAS generally is not used as a major source of water supply because of the relatively low yields to wells (< 19 L/min), high Fe content, and the potential for contamination. The IAS consists of several water-bearing units separated by confining units, which are composed mainly of the siliciclastic Hawthorn Group with interlayered sequences of more and less permeable carbonates, sands and clays. The extent, thickness, and permeability of the IAS are variable, but generally control the

downward leakage between the SAS and the UFA (Katz et al., 2009). The UFA is the major source of water supply within the study area and consists of permeable limestone and dolomite deposited in a shallow marine environment (Miller, 1986).

2.2. Aquifer matrix

The median Mo and As concentrations in the IAS and UFA matrix were in the range between 2 and 3 mg/kg and varied significantly with depth (Pichler and Mozaffari, 2015) and their distribution was heavily skewed due to occasionally high values of up to 100 mg/kg for As and up to 880 mg/kg for Mo. The maximum concentrations within the control core DEP5 were 223 mg/kg for Mo and 56 mg/kg for As. In the shallow SAS where the conditions are more oxygenated, As is likely bound to hydrous ferric oxide (HFO) phases, i.e., ferrihydrite, while in the deeper UFA where Fe and S are elevated, As is mainly present as an impurity in pyrite with concentrations of up to 9000 mg/kg (Pichler and Mozaffari, 2015). The exact mineralogical association of Mo in the aquifer matrix remains somewhat unclear, since electron microprobe analyses of pyrite did not confirm the presence of Mo in pyrite. Instead the likely primary source for Mo is organic matter. Organic matter (OM) was found throughout the aquifer matrix ranging from 0.1 to 3.3 % with a median concentration of 1.4 %. Molybdenum, however seemed to be only loosely bound to mineral and organic matter surfaces, since it was easily removed from the aquifer matrix during a single step liquid extraction at pH 8.1 (Pichler and Mozaffari, 2015).

3. Material and methods

3.1. Sample collection

Water samples were collected from the DEP wells five times over a one year period following National Water-Quality Assessment (NAWQA) protocol (Koterba et al., 1995). Each well was purged a minimum of three casing volumes before collection of water samples, although readings of temperature, pH, specific conductance, and dissolved oxygen generally stabilized earlier. The purged volumes ranged from approximately 180 L for the shallow wells to 400 L for the deepest wells. Immediately following well installation and well development in April 2008 field parameters and As and Mo were analyzed. At all other times, i.e., May 2008, June 2008, October 2008 and April 2009 the full suite of elements was analyzed. Sulfide was determined in the field on a Hach DR 2800 VIS Spectrophotometer. Molybdenum (Mo) was analyzed on a Perkin Elmer Optima 2000 DV inductively coupled plasma – optical emission spectrometer (ICP-OES). Total As and As species (arsenite and arsenate) were analyzed by hydride generation – atomic fluorescence spectrometry (HG-AFS) following Price et al. (2007). The accuracy and precision of the measurements were verified through the use of internal and external standards; analytical uncertainty was depended on the absolute concentration of each element, but always better than 5 %. All other chemical parameters were analyzed by the certified laboratory of the Florida Department of Environmental Protection (FDEP) by a combination of ion chromatography (IC), ICP-OES and ICP-MS.

3.2. Numerical model approach and model setup

Based on the mineralogical and hydrogeological site characterization and the observed hydrochemical changes of groundwater following the drilling and installation of monitoring wells, conceptual flow and processes models were formulated. They were implemented numerically using the USGS code MODFLOW in conjunction with the reactive multicomponent transport code PHT3D (Prommer et al., 2003), which incorporates PHREEQC-2 (Parkhurst and Appelo, 1999) for the geochemical calculations. The models were set up to compare the hydrochemical response in the area of elevated (DEP4) and low Mo and As concentrations (DEP5). Flow models simulated a period of 365 days, commencing with the drilling phase, approximated through ingress of oxygen-saturated groundwater into the aquifer at a rate of 1 m^3/d. The latter provided an estimate of realistic water volumes lost to the aquifer during drilling. Thereafter the system was returned to undisturbed (pre-drilling) hydrological conditions, characterized by its 'ambient' groundwater flow velocity (Fig. 1). The system was only disturbed due to sampling on day 3, 33, 63, 186 and 365 of the simulation period, through removal of approximately 3 well volumes of groundwater.

As the water loss to the aquifer during drilling operations was small compared to the natural background flow in this high permeability aquifer, its impact on ambient flow directions and velocities was assumed to be negligible (< 5 % during the drilling phase based on ambient groundwater flux estimates). Subsequently, a 2D model was set up parallel to the flow direction. The aquifer was assumed to be homogeneous in its lateral direction and simulated over a horizontal extent of 50 m, with constant head boundaries enforcing the average ambient hydraulic gradient within the aquifer. The upstream boundary was selected such that it was sufficiently far from the monitoring well to not impact solute concentration fronts during the one-year simulation period. Cell sizes varied from 0.1 m at the monitoring well to 1 m at the outer edges of the model domain. The depth horizon targeted by the simulated monitoring well was separated into 20 layers. The hydrogeological model and initial parameter estimates were based on sedimentological characteristics of the aquifer (Table 1).

Based on the flow models, reactive transport models were set up to evaluate and quantify the mobilization, transport and sorption of As and Mo, as well as related redox reactions. Available data for the aquifer matrix, groundwater flow and groundwater composition (Table 1) were used for the development of the reaction network.

3.2.1. Reaction network

Based on the existing data, the key driver for the observed changes in the monitoring wells was postulated to be the ingress of oxygen into the aquifer due to aerated drilling fluids. That in turn was postulated to lead to the mineralization of sediment-bound organic matter and the dissolution of pyrite. The general formula CH_2O was chosen to represent the generalized bulk organic matter composition and was put into the model according to the measured sediment-bound organic matter concentrations. Biodegradation of organic matter was represented by standard Monod-type rate expressions (Barry et al., 2002; Greskowiak et al. 2006):

$$r_{om} = \left[r_{ox}\left(\frac{C_{ox}}{2.9x10^{-4} + C_{ox}}\right) + r_{nitr}\left(\frac{C_{nitr}}{1.55x10^{-4} + C_{nitr}}\right) \times \left(\frac{k_{ox\ inh}}{k_{ox\ inh} + C_{ox}}\right) + r_{sul}\left(\frac{C_{sul}}{1.0x10^{-4} + C_{sul}}\right) \times \left(\frac{k_{ox\ inh}}{k_{ox\ inh} + C_{ox}}\right) \times \left(\frac{k_{nitr\ inh}}{k_{nitr\ inh} + C_{nitr}}\right) + r_{Fe}\left(\frac{C_{Fe}}{1.0x10^{-6} + C_{Fe}}\right) \right] \quad (1)$$

where r_{om} is the overall degradation rate of organic matter, r_{ox}, r_{nitr}, r_{sul} and r_{fe}, are the maximum rate constants of carbon mineralization under aerobic, denitrifying, sulfate- and iron reducing conditions, respectively. C_{ox}, C_{nitr}, C_{sul}, and C_{Fe} are the concentrations of DO, nitrate, sulfate and Fe-oxides respectively and $k_{ox\ inh}$ and $k_{nitr\ inh}$ are inhibition constants. Additional Monod terms for organic matter were not included, assuming that OM was not depleted during the simulation time.

Pyrite oxidation by oxygen was included based on the rate expression by Williamson and Rimstidt (1994), extended by additional oxidation with nitrate as previously proposed and applied by Eckert and Appelo (2002):

$$r_{pyr} = \left[\left(C_{O_2}^{0.5} + f2C_{NO_3^-}^{0.5} \right) C_{H^+}^{-0.11} \left(10^{-10.19} \frac{A_{pyr}}{V} \right) \left(\frac{C}{C_o} \right)_{pyr}^{0.67} \right] \quad (2)$$

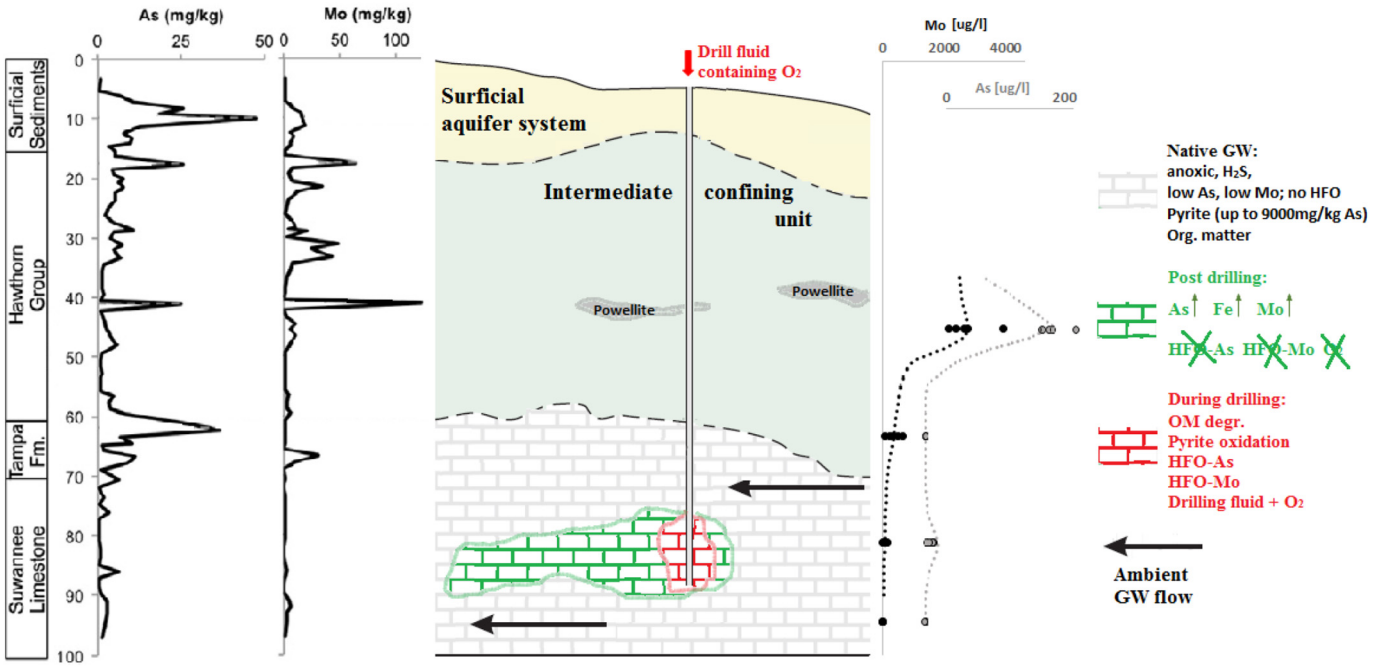

Fig. 1. Diagram of the hydrochemical conceptual model of the aquifer response to drilling in the Upper Floridan Aquifer, where background concentrations of As and Mo are low. During drilling ingress of oxygen triggers redox reactions and a zone of pyrite oxidation and OM degradation ensues (red zone). Post drilling elevated As and/or Mo concentrations spread into the aquifer in accordance to the ambient groundwater velocity (green zone). Also shown is the hydrostratigraphic sequence of the tertiary aquifer, the As and Mo solid phase and dissolved phase concentrations at site DEP2 with depth (data from Pichler and Mozaffari, 2015). (For interpretation of the references to colour in this figure legend, the reader is referred to the web version of this article.)

where r_{pyr} is the specific oxidation rate for pyrite. C_{O2}, C_{NO3-} and C_{H+} are the oxygen, nitrate and proton groundwater concentrations, A_{pyr}/V is the ratio of mineral surface area to solution volume and c/c_o is a factor that accounts for changes in A_{pyr} resulting from the progressing reaction. F_2 is a constant, which was assumed to be unit, as in previous work (Eckert and Appelo, 2002).

In addition, calcite ($CaCO_3$), ferrihydrite ($Fe(OH)_3$), siderite ($FeCO_3$) and powellite ($CaMoO_4$) were included at measured concentrations and allowed to dissolve and/or precipitate according to equilibrium assumptions. Thermodynamic data for powellite was added to the PHREEQC database on the basis of investigations into the calcium molybdate solubility by Essington (1990), while data for aqueous Mo speciation was based on the compilation by Carroll et al. (2006), which in turn was based on laboratory experiments by Smith and Martell (1976), Kaback and Runnells (1980) and Essington (1990).

3.2.2. As and Mo release

The oxidative dissolution of As-rich pyrite was considered the primary reason for elevated As concentrations following well drilling. Prior to drilling, pyrite was in thermodynamic equilibrium with the reducing native groundwater and ferrihydrite was under-saturated in all simulated horizons (Table 1). With the commencement of drilling and the ingress of aerated drilling fluids, redox conditions temporarily changed towards oxic conditions, triggering pyrite dissolution. Within the model, As release was stoichiometrically linked to the computed pyrite oxidation rate, as done previously (Wallis et al., 2010) with a molar ratio of As to FeS_2 based on the aquifer matrix analysis (Table 1).

The mineralization of OM and the dissolution of powellite ($CaMoO_4$) were considered the potential cause for elevated Mo concentrations following drilling. Pyrite was dismissed as a potential source, since Mo was not detected in pyrite in the UFA. Within the model, Mo was incorporated as a minor constituent in OM based on measured OM and Mo concentrations, adjusted during model calibration (Table 1).

3.2.3. Surface complexation

Sorption of arsenic and molybdenum was included as a surface complexation reaction with $Fe(OH)_3$. The generalized two-layer surface complexation model of Dzombak and Morel (1990) was employed, extended by reactions for Fe^{2+}, HCO_3 and Si (Appelo et al., 2002; Swedlund and Webster, 1999). In addition, the potential complexation of Mo onto ferrihydrite was included based on Gustafsson (2003) and a compilation of laboratory batch experiments of Mo adsorption by Carroll et al. (2006). That allowed competitive sorption between As and Mo and other ions for a finite number of sorption sites.

The successively increasing and decreasing sorption capacity with precipitation and dissolution of $Fe(OH)_3$ following drilling was modelled by coupling the moles of the surface complex to the mass of $Fe(OH)_3$ in the aquifer. The properties of ferrihydrite were defined according to the values proposed by Dzombak and Morel (1990), that is, weak and strong site densities were 0.2 and 0.005 mol/mol of ferrihydrite, respectively, and a surface area of 600 $m^2\ g^{-1}$.

4. Results and discussion

4.1. Observed temporal changes in elemental concentrations

Concentrations for all analyzed parameters are presented in Table S1. The major ions Na, Mg, K, Si and Cl remained constant within their analytical uncertainty of better than 5 % throughout the sampling period. That was expected, since drilling fluid and Lithia groundwater had approximately the same major ion concentrations. Arsenic (As) values were generated by two laboratories, the FDEP laboratory and the USF Center for Water Analyses, since As showed a most erratic behavior and without confirmation by two independent laboratories there would have been doubt about the data quality. There was excellent agreement between the two data sets ($r^2 = 0.99$). With the exception of well DEP1-1, three different developments with respect to As

Table 1
Parameters for the transport model and the charge-balanced and equilibrated aqueous components and minerals for sites DEP4-2 and DEP5-1 and corresponding literature values.

Equilibrated and charge balanced initial model concentration (mmol L^{-1})[a]		
	DEP5-1	DEP4-2
pH	7.6	7.7
pe[b]	−4.4	−4.54
O_2	–	–
TIC	3.1	3.0
CH_4	$4.9 * 10^{-3}$	$1.5 * 10^{-3}$
Ca	1.03	0.93
K	$2.3 * 10^{-2}$	$3.8 * 10^{-2}$
Na	0.35	0.47
Cl	0.23	0.17
Fe^{2+}	$9.8 * 10^{-4}$	$1 * 10^{-3}$
Mg	0.58	0.5
Si	0.45	0.4
SO_4	$4.5 * 10^{-2}$	0.12
F	$2.1 * 10^{-2}$	$2.1 * 10^{-2}$
Mo	$5 * 10^{-6}$	$3.4 * 10^{-4}$
As	$9 * 10^{-6}$	$7 * 10^{-5}$
Saturation state of minerals in contact with ambient groundwater		
SI $_{Fe(OH)3}$	−5.86	−6.69
SI $_{pyrite}$	0.61	9.45
SI $_{siderite}$	−0.8	−0.80
SI $_{powellite}$	−8.6	−2.00

Mineral phases and solid trace metal concentrations

Solid phase	Units	Value	Lit. value	Source
Powellite ($CaMoO_4$)	(mol L_{bulk}^{-1})	0	–	Pichler and Mozaffari (2015)
Ferryhydrite ($Fe(OH)_3$)	(mol L_{bulk}^{-1})	0	–	Pichler and Mozaffari (2015)
Calcite ($CaCO_3$)	(mol L_{bulk}^{-1})	0.5	–	Pichler and Mozaffari (2015)
F^- in calcite ($Ca(CO3)_yF_x$)	(mg/kg)	1143	–	Model calibration
As in pyrite	(mg/kg)	< 100 to 11,200	300 to 9000 100 to 11,200	Pichler and Mozaffari (2015), Price and Pichler (2006)
Pyrite	(mg/kg)	1000	276 to 32,406	Price and Pichler (2006)
Org. matter (median)	(wt%)	1.4	0.1 to 3.3 wt%	Pichler and Mozaffari (2015)
Mo concentration in IAS, UFA[c]	(mg/kg)	224 in org matter	< 0.5 to 880	Pichler and Mozaffari (2015)
Model parameters				
n_e	(−)	0.25	–	–
α_L[d]	(m)	0.05	–	–
α_T[d]	(m)	0.005	–	–
Grid cell size	(m)	0.1–1	–	–

[a] Except temperature in (C°), minerals in (mol L^{-1} of bulk aquifer volume) and pH, pe.
[b] Initial pe based on PHREEQC calculation of equilibrated and charged balance native groundwater chemistry.
[c] Intermediate Aquifer System (IAS), and the Upper Floridian Aquifer System (UFA).
[d] α_L = longitudinal dispersivity; α_T = transverse dispersivity.

concentration were observed between April 2008 and April 2009 (Fig. 2a and Table S1):

(1) wells with ambient As concentrations above 150 μg/L (DEP2-1 and DEP3-1), showed increasing concentrations with time,
(2) wells with ambient concentrations between 10 μg/L and 50 μg/L (DEP1-3, DEP3-3, DEP4-1 and DEP4-2) showed first an increase, followed by a constant decline, while wells with ambient concentrations between 2 μg/L and 3 μg/L (DEP4-3, DEP5-1 and DEP5-3) showed a constant decline,
(3) wells with ambient concentrations below 1 μg/L showed no significant trend with time.

The only exception was well DEP1-1, which had up to 99 μg/L As, but showed no discernible trend.

With respect to Mo concentrations the following was observed (Fig. 2b and Table S1):

(1) wells DEP2-1 and DEP3-1, which had above 3000 μg/L Mo showed increasing concentrations with time,
(2) well DEP4-1, which had up to 131 μg/L Mo did not show any trend,
(3) all other wells regardless of initial Mo concentration showed a constant concentration decline.

Hence, the initial concentrations in wells with increasing As and Mo concentrations were interpreted to be 'false negatives', while the initial concentrations in wells with decreasing As and Mo concentrations were interpreted to be 'false positives'.

The observed trends could have been caused by an overall change in hydrogeochemical conditions over the course of the investigation. That possibility, however, was deemed unlikely since none of the 90 private supply wells in the Lithia area, which were sampled in December 2007, May 2008 and April 2009 underwent systematic changes in physico-chemical conditions or in As and Mo concentrations (Pichler et al., 2017).

The likely explanation for the increasing trends of As and Mo in wells DEP2-1 and DEP3-1 would be mixing of groundwater with drilling fluid and potentially adsorption by ferrihydrite, which precipitated due to introduction of oxygen into the aquifer (Brunsting and McBean, 2014). An additional explanation could be that installation of the well triggered geochemical reactions, which caused an increase of As and Mo release from the aquifer matrix with time. That, however, was ruled out since

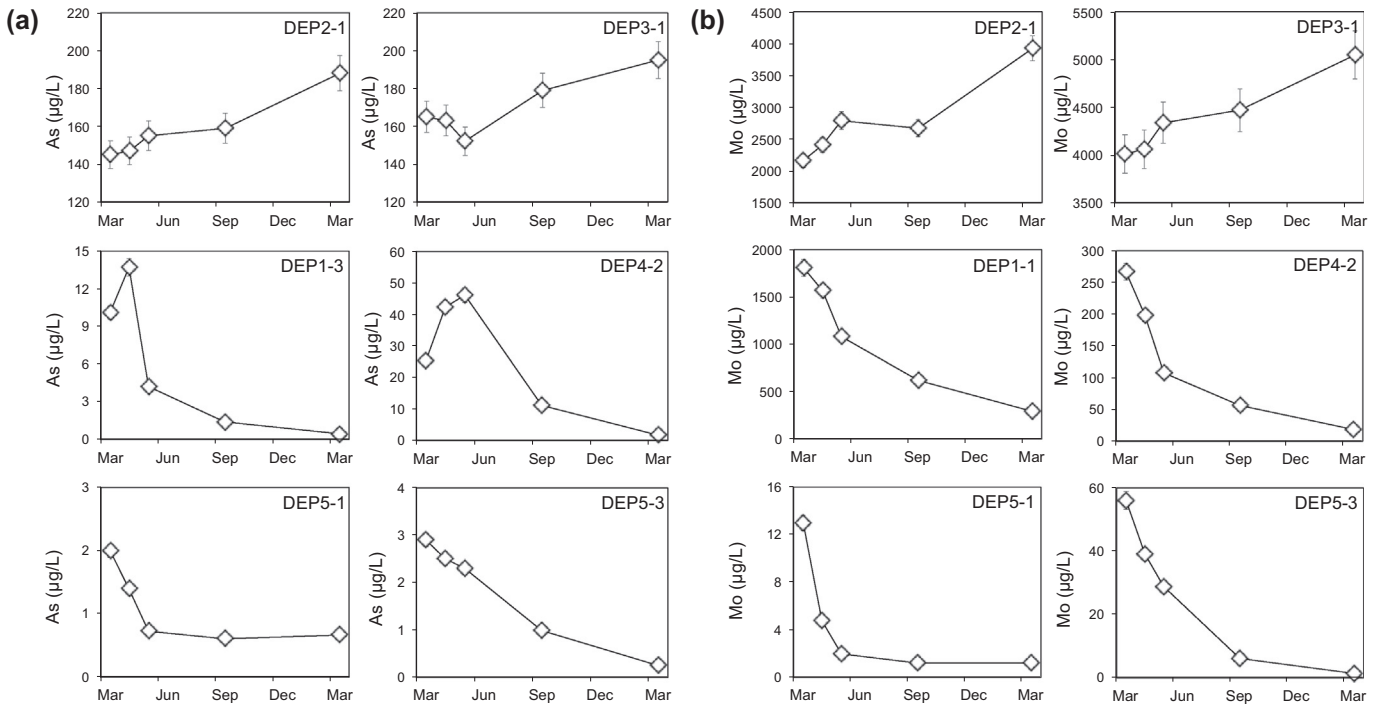

Fig. 2. (a) Changes in arsenic (As) concentrations and (b) changes in molybdenum (Mo) concentrations from April 2008 to April 2009 in selected monitoring wells in the Lithia area, central Florida. Analytical uncertainty of 5 % is represented by error bars or is smaller than the marker itself.

As and Mo concentrations in many private supply wells from the same hydro-stratigraphic horizon were higher than those observed in DEP2-1 and DEP3-1 (Pichler et al., 2017). Furthermore, at the monitoring depth of DEP2-1, As and Mo concentrations in the aquifer matrix were relatively low and in the case of As apparently difficult to mobilize (Fig. 3). Pichler and Mozaffari (2015) reported that only 20 % of already relatively low As values were mobilized from the corresponding aquifer matrix, while Mo concentrations were comparable to those at the control site (DEP5) (Fig. 3).

Precipitation of ferrihydrite immediately after well installation due to the input of oxygen could theoretically induce an increasing trend, because initially As and Mo could have been removed from groundwater due to adsorption followed by its release as conditions change back to reducing (e.g., Brunsting and McBean, 2014). In Lithia, however, ferrous iron (Fe^{2+}) concentrations in the aquifer are low and do not change enough for ferrihydrite precipitation to remove As and Mo sufficiently. For example, in well DEP2-1, Fe^{2+} changed by about 50 µg/L, which would allow for the sorption of approximately 33 µg/L As under

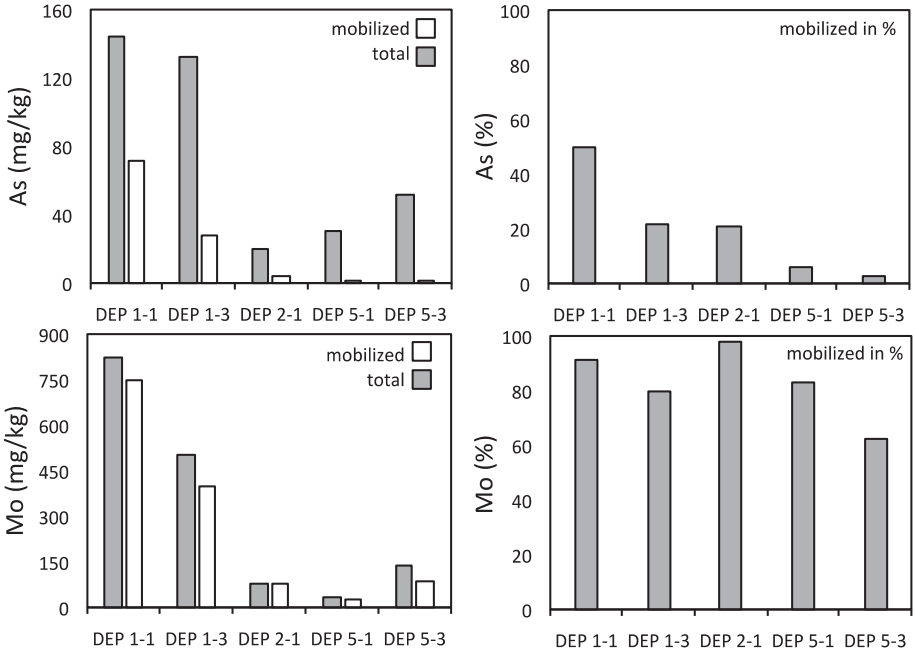

Fig. 3. Absolute and relative amounts of Mo and As leached due to reaction with a NaOAc solution at pH 8.1 from drill core samples collected during the installation of monitoring well clusters in the Lithia area. The sample names correspond to the monitoring well intervals (data from Pichler and Mozaffari (2015)).

ideal conditions, where the molar Fe/As ratio in ferrihydrite could be as low as 2 (Brunsting and McBean, 2014). However, As changed by 41 μg/L, leaving 20 % of the As and 100 % of the Mo unaccounted for. Thus, as anoxic conditions resume rapidly after drilling, prolonged stability of ferrihydrite and thus sustained release from sorption sites was deemed unlikely under the prevailing redox conditions and because $^{-}Fe^{2+}$ concentrations in the aquifer were too low, precipitation of ferrihydrite, was not considered as a major process for the removal of As and Mo in the Lithia area. That suggested dilution of already contaminated groundwater with As and Mo free drilling fluid as the main process for the increasing trend in As and Mo concentrations, with a minor component due to precipitation of ferrihydrite.

The initial increase of As in those wells where overall the As concentration declined with time (Fig. 2a) should be related to the mineralogy in the aquifer matrix. In the Floridan aquifer system As is generally found as impurities in pyrite (e.g., Lazareva and Pichler, 2007; Pichler et al., 2011), which undergoes oxidative dissolution until oxygen is consumed, leading to observed As concentration peaks following drilling (Fig. 2a). Then as the physicochemical conditions in the aquifer return to anoxic, As concentrations also return to concentrations well below the current drinking water standard of 10 μg/L. The maximum attained As peak concentrations are thereby found to correlate to the mobility and abundance of As observed during the leaching experiments carried out by Pichler and Mozaffari (2015), which closely mimicked the conditions during and immediately after well installation, i.e., interaction with an oxygen saturated solution (Fig. 3). The two wells at the DEP5 site showed generally low As peak concentrations followed by a constant decline to values below 1 μg/L. Apparently in the corresponding aquifer matrix for DEP5-1 and DEP5-3 As is of low abundance and not as easily removed as for example in DEP1-3 (Fig. 3). Thus, comparison between As concentrations in groundwater collected from the DEP wells (Fig. 2a) and leachability of As from the corresponding aquifer matrix (Fig. 3) allowed the conclusion that when As was abundant and easily leachable higher concentrations resulted and when abundance was low and/or leachability was low overall lower concentrations resulted due to well installation.

Compared to As, the mobility of Mo was more susceptible to well installation since with the exception of DEP4-1 and the two high-Mo wells all other wells showed a declining trend with time (Fig. 2b and Table S1). This should indicate that generally Mo was more mobile than As, which was also observed during the leaching experiments carried out by Pichler and Mozaffari (2015). Under the same experimental conditions as for As, Mo removal from the aquifer matrix was much stronger with removal rates consistently above 60 % (Fig. 3). Thus, Pichler and Mozaffari (2015) concluded that Mo in the aquifer matrix had to be only loosely bound to mineral and organic matter surfaces, particularly since Mo was not found to be present in pyrite, which in turn is in agreement with the same observations made by Chappaz et al. (2014). Organic matter is known to be an important reservoir for Mo (Wichard et al., 2009;Tribovillard et al., 2004, Helz et al., 2011, Chappaz et al., 2014) with some proposing the degradation of organic matter to be the main source of Mo in porewaters (Contreras et al., 1978). Hence Mo should be more mobile than As, which would explain why changes in Mo concentrations were much more susceptible to well installation.

In addition to total dissolved As concentrations in groundwater, As was speciated into its two common redox species, arsenite (As(III) and arsenate As(V)). Except for samples from well DEP1-1 the sums of As species and the As total concentrations were in good agreement. The observed deviation in DEP1-1 was caused by the high pH in those samples, which affected the speciation analyses. Deviations of > 15 % in other samples could have been caused by the presence of thio arsenic species (e.g., Planer-Friedrich et al., 2007), which were not analyzed. When detected, the abundance of As(V) decreased consistently with time and hence the As(V)/As(III) ratio was showing the change in redox conditions from oxidizing to reducing. This was also accompanied by an increase in sulfide (HS^{-}) for most wells (Table S1). Iron (Fe) concentrations showed similar trends to As and Mo in several wells. Concentrations, however were often in the vicinity of 30 μg/L, the detection limit of the analytical method and have to be regarded with caution. In summary, the observed concentration and redox trends cannot be attributed to natural changes in the aquifer beneath Lithia, they have to be an artefact of well installation. This proposition was investigated in detail using data-constrained reactive transport modelling.

4.2. Quantification of key redox processes

The data-constrained flow and reactive transport model provided a detailed description of the key processes that influence the temporal changes in major ion and redox groundwater chemistry following drilling, which are discussed exemplary for monitoring well DEP4-2 (Fig. 4). The observed and simulated concentration patterns of major and minor ions, in conjunction with the measured calcite, pyrite, powellite and organic matter phase concentrations suggested that the oxidation of pyrite and OM mineralization exerted a strong influence on solution redox chemistry. The temporal supply of electron acceptors in the form of dissolved O_2 at the time of drilling triggered pyrite oxidation and organic matter mineralization leading to the observed and simulated increase in SO_4 and total inorganic carbon (TIC) concentrations and the simultaneous depletion of O_2 (Fig. 4). The gain in Fe, SO_4 and TIC concentrations thereby provided an effective model constraint for the rate and amount of pyrite dissolution and organic matter mineralization.

Ferrous iron present in the ambient groundwater, but also freshly produced following pyrite dissolution, precipitated as ferrihydrite (HFO). The zone of pyrite and OM dissolution and ferrihydrite precipitation (the 'redox reaction zone' (RRZ)) was thereby restricted to the proximity of the monitoring well (< 1.3 m), given the short duration of oxygen supply and the rapid O_2 consumption rate (average 0.08 μmol/L/min). Subsequently, the cumulative amounts of dissolved pyrite and precipitated ferrihydrite, constrained on the basis of Fe and SO_4 concentrations, remained low— (Fig. 4). Siderite remained under saturated throughout the simulation.

The mineralization of OM and an associated increase in CO_2 led to enhanced dissolution of calcite around the well (Fig. 4), which was accompanied by elevated fluoride concentrations. As groundwater remained under saturated in respect to calcium fluoride (CaF_2), it is speculated that fluoride, known to adsorb to calcite mineral surfaces, was released during dissolution of $CaCO_3$ (e.g. Turner et al., 2005). A fluoride concentration within calcite of 1143 mg/kg allowed peak concentrations to be replicated (Table 1 and Fig. 4).

The time it took for anoxic conditions to return was controlled by the background flow velocity and the redox condition of the ambient groundwater and was constrained by diminishing O_2 and steadily rising HS^{-} concentrations (Fig. 4). The increase of anoxic groundwater within the redox reaction zone halted pyrite and OM oxidation within 1 month of drilling and caused the dissolution of ferrihydrite, which formed immediately after well installation (Fig. 4).

4.3. Quantification of Mo and As source term

The simulations confirmed that the observed temporal dynamics of As and Mo mobilization were controlled by release of As, Mo and Fe during pyrite oxidation and OM mineralization under oxic conditions (Fig. 4). The simulated OM degradation rate was thereby on average 2 orders of magnitude higher than that of pyrite, i.e., 1.5 mmol C/L/yr and 0.009 mmol/L/yr, respectively. Those rates were comparable to reported literature values (Jacobsen and Postma, 1994; Xu et al., 2008). As a result, Mo was generally released at a faster rate than As. In addition, sorption to ferrihydrite temporarily slowed As release, while Mo was relatively unaffected due to its lower sorption affinity. Subsequently, secondary trace metal release during ferrihydrite dissolution during the return to anoxic conditions was only of significance for As

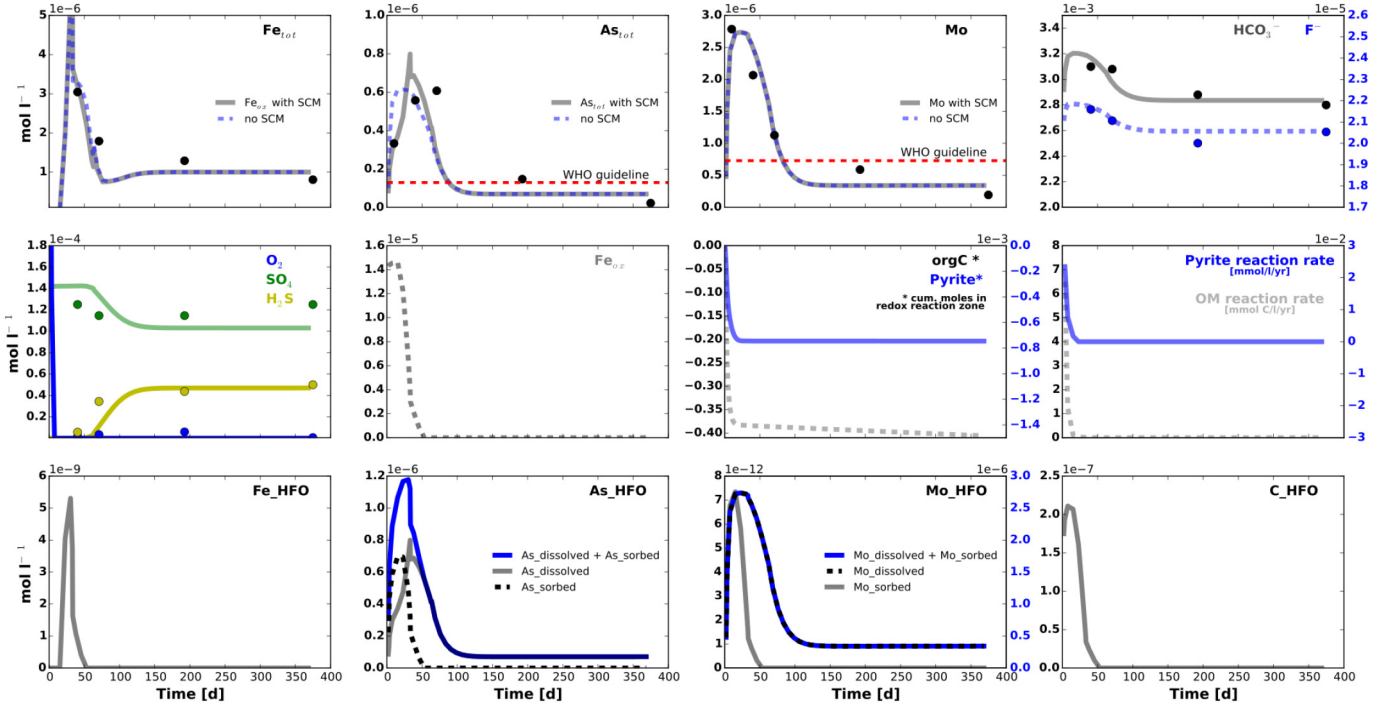

Fig. 4. Measured (circles) and simulated (solid/dashed lines) aqueous concentrations of selected ions over 365 days in drilling horizon DEP4-2. SCM = surface complexation model.

(Fig. 4). As a consequence, the relative mobility of As was lower than that of Mo and attainment of As peak concentrations was delayed compared to Mo and Fe (Fig. 4). Comparative model runs (not shown) demonstrated that the sooner anoxic conditions returned and ferrihydrite dissolved, the faster As peak concentrations were attained, diminishing the delay between maximum As and Mo levels.

Arsenic concentrations in pyrite of 0.53 wt% replicated the measured As peak concentrations in wells outside the area of contamination (Fig. 5, DEP5-1), while in areas of naturally elevated As and Mo concentrations (DEP1 to 4) solid phase As concentrations in pyrite could be considerably higher. Observed aqueous As to Fe molar ratios as high as 1:3 (Fig. 4, DEP4-2) were only replicated at As concentrations above those measured in pyrite (max. 1.12 wt%, see Table 1). Thus, similarly to Mo some of the mobilized As may have been present in OM (e.g., Lin et al., 2017) (Fig. 5). Organic matter is known to serve as a binding agent for As, however, comparably little research has been done on any quantification (e.g., Wang and Mulligan, 2006). The most likely scenario for an additional source, however, was that occasionally As occurred adsorbed to clay minerals, as demonstrated for the UFA by Price and Pichler (2006). Other potential hosts for As, i.e. ferrihydrite and powellite were rejected as a source of As since they were not thermodynamically stable at ambient groundwater conditions.

Peak concentrations of Mo that were measured outside of the area of contamination (DEP5-1) were replicated assuming that all Mo was present in OM at a concentration of 0.3 wt%, a value consistent with measured concentrations of up to 224 mg/kg in the aquifer matrix (Table 1 and Fig. 5). However, model simulations indicated that the Mo:OM ratios could be elevated in the area of known contamination, analogous to the potentially higher As:FeS_2 ratios in those regions (max. 4 wt% for DEP4-2, Fig. 5). A subsequent quantification of the abundance of As and Mo in their respective host phases through modelling on the basis of Fe, As and Mo concentrations from an additional two monitoring horizons (DEP4-4 and DEP3-1) highlighted their variability in the aquifer matrix and explained why Mo and As concentrations in

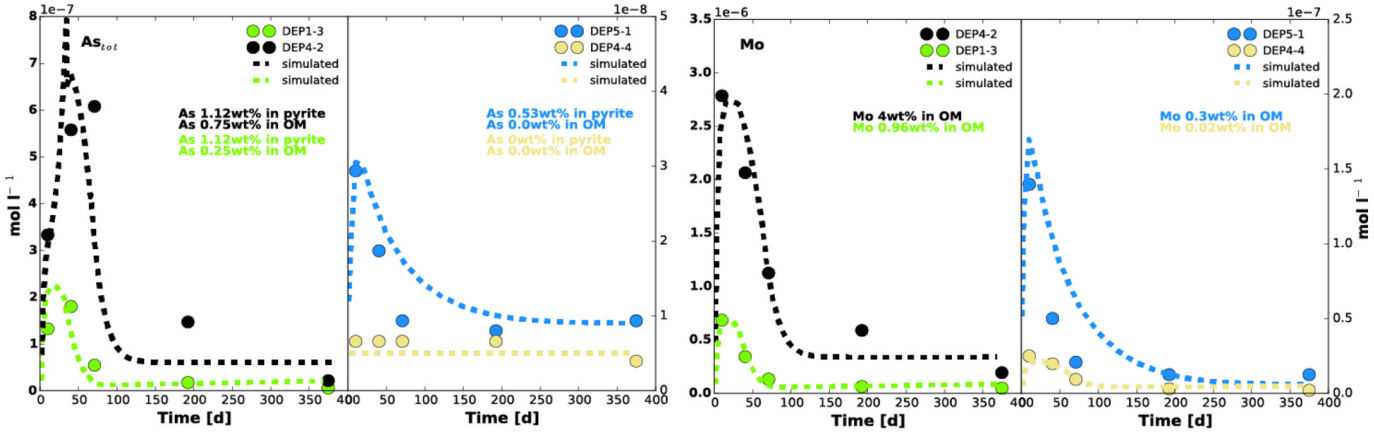

Fig. 5. Fe, As and Mo concentrations for DEP5-1, DEP1-3, DEP4-2 and DEP4-4 (simulated = broken line, observed = circle). Simulated abundances of As and Mo in pyrite and organic matter are given as wt%.

the monitoring wells varied from site to site despite similar redox conditions (Fig. 5).

4.4. Spatial and temporal dynamics of arsenic and molybdenum concentrations

Following primary (pyrite and OM) and secondary (ferrihydrite) release, As and Mo migrated downgradient and concentrations dissipated during aquifer passage due to mixing and dispersion. Under the ambient groundwater velocities, no As or Mo breakthrough (> 10 μg/L) occurred beyond 30 m downstream of the monitoring bore in any of the simulated sites. The persistence of elevated As and Mo concentrations at the monitoring bore is thereby largely controlled by the groundwater flow velocity as comparative model runs demonstrate (Fig. 6). In addition, geochemical reactions under the returning reducing conditions such as co-precipitation with pyrite could accelerate the decrease in As and Mo concentrations.

Therefore, modelling suggests that the zone of elevated concentrations is restricted to the immediate vicinity of the drilled bore and that natural attenuation of elevated concentrations is achieved within acceptable transport distances and time frames. It is noteworthy, however, that occurrence of preferential flow paths may provide exposure pathways to potential receptors at greater distances from the monitoring bore.

4.5. Model limitations

While the dominant redox processes and the subsequent mobilization of As and Mo are well described by the model, it should be noted, that several model assumptions were likely oversimplifications. Firstly, the data was obtained during routine monitoring to ensure that groundwater at the site met state and federal drinking-water-quality criteria. The available geochemical dataset is therefore comprehensive, however, more frequent analysis immediately following drilling would have provided additional constraints for model calibration. As the drilling itself was not under investigation, data gaps exist in regards to the exact amount of drilling fluid used and the ambient groundwater velocities. The latter were not explicitly measured at each well but were inferred on the basis of potentiometric head measurements. Consequently, the mineral dissolution rates and molar ratios of As and Mo in pyrite and organic matter, which were quantified as part of this study also remained indicative only. Also, small-scale, processes in the immediate vicinity of the well were simplified, such as the mode of oxygen ingress being restricted to advective transport of dissolved oxygen neglecting gaseous diffusion and the representation of the aquifer mineral assemblage as being homogenous. Despite these limitations, the available mineralogical and geochemical data in conjunction with the developed model was able to provide valuable insights into the coupled flow and reaction patterns that can affect not only As and Mo, but also the release of other trace metals from redox sensitive phases. It raises awareness of the possibility of temporarily altered concentrations as a consequence of drilling and improves our ability to critically evaluate the 'representativeness' of monitoring data.

5. Conclusions

The presented data demonstrated drilling induced As and Mo mobilization, while the reactive transport simulations reconstructed the spatial and temporal hydrochemical changes that occurred following well installation. Thus, installation of a monitoring well in the context of groundwater contamination can lead to the following two scenarios: (1) relatively lower concentrations ('false negatives') and (2) relatively higher concentrations ('false positives'). If a contaminant is present in groundwater and absent in the drilling fluid, then relatively lower contaminant concentrations are likely the result of dilution, i.e., mixing between groundwater and drilling fluid. Precipitation of, for example, ferrihydrite may also remove As or Mo if the ambient groundwater is Fe-rich. If a potential contaminant is present as a redox sensitive mineral or as an impurity in a redox sensitive mineral, then introduction of oxygen into the aquifer via the drilling fluid can cause its release and lead to relatively higher concentrations. With time, however, concentrations will return to their actual, pre-installation concentration. Unfortunately, it is close to impossible to predict the exact time required, but based on the observations presented here it seems likely that the higher the initial concentrations the longer the period.

In the study area, As and Mo were mainly present in the aquifer matrix either as an impurity in pyrite or adsorbed by organic matter (OM), both of which are not thermodynamically stable under oxidizing conditions. The data-constrained reactive transport model simulations confirmed that the drilling-induced oxidation of pyrite and OM mineralization triggered the release of As and Mo, explaining the 'false positive' observations. Chemical data and modelling highlighted the fact that Mo and As concentrations can vary markedly in the aqueous phase from site to site despite similar redox conditions. This variation is directly linked to the As and Mo abundance in the aquifer matrix, i.e., if As and Mo were high in the aquifer matrix concentrations were also high in the monitoring wells. While As is generally present in pyrite, the simulation of its concentration in the aqueous phase required an additional source, most likely clay or possibly OM, if concentrations were high.

Natural attenuation of elevated As and Mo concentrations was achieved within relatively short transport distances (< 30 m), due to mixing and dispersion with the ambient groundwater. Elevated trace metal concentrations at the monitoring well returned within one year

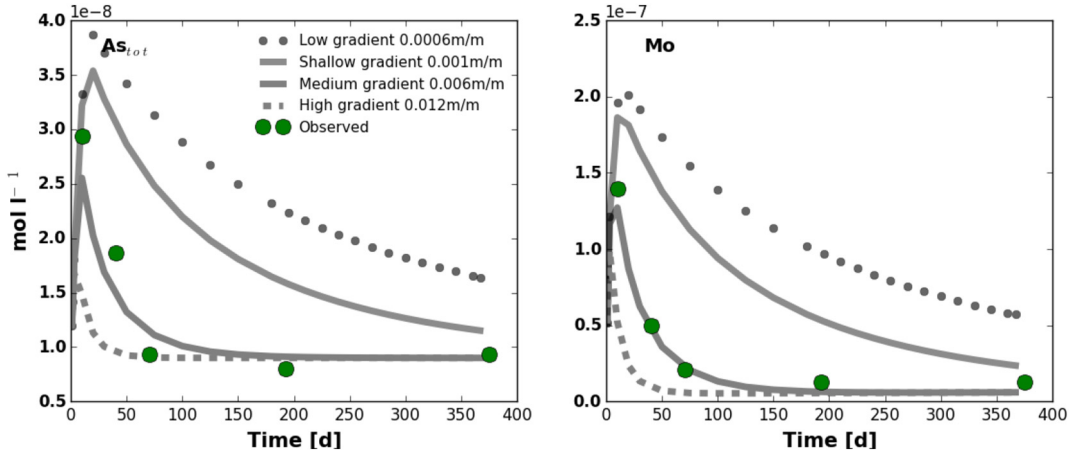

Fig. 6. Temporal evolution of trace metal concentrations under varying background flow velocities in well DEP5-1.

back to background concentrations, however model simulations show, that under low or no-flow conditions, elevated concentrations could persist over prolonged periods of time.

Supplementary data to this article can be found online at https://doi.org/10.1016/j.scitotenv.2018.03.063.

Acknowledgments

We thank the Florida Department of Environmental Protection Site Investigation Section who made this study possible. Particularly participation by Jeff Newton, Robert Cilek and William Martin was greatly appreciated. Part of the work was funded through a grant from the German Research Foundation (DFG-Projekt PI 746/1-1) to Thomas Pichler. Thomas Pichler also acknowledges support in form of a fellowship from the Harris German Distinguished Visiting Professorship Program at Dartmouth College.

References

Appelo, C.A.J., Van der Weiden, M.J.J., Tournassat, C., Charlet, L., 2002. Surface complexation of ferrous iron and carbonate on ferrihydrite and the mobilization of arsenic. Environ. Sci. Technol. 36 (14), 3096–3103.

Barry, D.A., Prommer, H., Miller, C.T., Engesgaard, B.A., Knudegaard, P., Brun, A., Zheng, C., 2002. Modelling the fate of oxidisable organic contaminants in groundwater. Adv. Water Resour. 25 (8–12), 945–983.

Bennett, D.B., Busacca, M., Clark, E.E., 1988. The modified reverse-cirrculation air rotary drilling technique for development of observation and monitoring wells at groundwater contamination sites. In: Collins, A.G., Johnson, A.I. (Eds.), Ground-water Contamination: Field Methods, Volume ASTM STP. Vol. 963. ASTM, Philadelphia, pp. 137–145.

Brunsting, J.H., McBean, E.A., 2014. In situ treatment of arsenic-contaminated groundwater by air sparging. J. Contam. Hydrol. 159, 20–35.

Carroll, K.C., Artiola, J.F., Brusseau, M.L., 2006. Transport of molybdenum in a biosolid-amended alkaline soil. Chemosphere 65, 778–785.

Chappaz, A., Lyons, T.W., Gregory, D.D., Reinhard, C.T., Gill, B.C., Li, C., Large, R.R., 2014. Does pyrite act as an important host for molybdenum in modern and ancient euxinic sediments? Geochim. Cosmochim. Acta 126, 112–122.

Contreras, R., Fogg, T.R., Chasteen, D., Gaudette, H.E., Lyons, B., 1978. Molybdenum in pore waters of anoxic marine sediments by electron paramagnetic resonance spectroscopy. Mar. Chem. 6 (4), 365–373.

Crimi, M.L., Siegrist, R.L., 2003. Geochemical effects on metals following permanganate oxidation of DNAPLs. Ground Water 41 (4), 458–469.

Dzombak, D.A., Morel, F.M.M., 1990. Surface Complexation Modeling. Wiley and Sons, New York, p. 1990.

Eckert, P., Appelo, C.A.J., 2002. Hydrogeochemical modeling of enhanced benzene, toluene, ethylbenzene, xylene (BTEX) remediation with nitrate. Water Resour. Res. 38 (8).

Essington, M.E., 1990. Calcium molybdate solubility in spent oil shale and a preliminary evaluation of the association constants for the formation of $CaMoO_4$(aq), $KMoO_4$-(aq), and $NaMoO_4$-(aq). Environ. Sci. Technol. 24, 214–220.

Greskowiak, J., Prommer, H., Massmann, G., Nuetzmann, G., 2006. Modeling seasonal redox dynamics and the corresponding fate of the pharmaceutical residue phenazone during artificial recharge of groundwater. Environ. Sci. Technol. 40 (21), 6615–6621.

Gustafsson, J.P., 2003. Modelling molybdate and tungstatead sorption to ferrihydrite. Chem. Geol. 200, 105–115.

Helz, G.R., Bura-Nakic, E., Mikac, N., Ciglenecki, I., 2011. New model for molybdenum behavior in euxinic waters. Chem. Geol. 284, 323e332.

Hughes, J.D., Vacher, H.L., Sanford, W.E., 2009. Temporal response of hydraulic head, temperature, and chloride concentrations to sea-level changes, Floridan aquifer system, USA. Hydrogeol. J. 17, 793–815.

Jacobsen, R., Postma, D., 1994. In situ rates of sulphate reduction in an aquifer (Romo, Denmark) and implications for the reactivity of organic matter. Geology 22, 1103–1106.

Jones, G.W., Pichler, T., 2007. The relationship between pyrite stability and arsenic mobility during aquifer storage and recovery in Southwest Central Florida. Environ. Sci. Technol. 41 (3), 723–730.

Kaback, D.S., Runnells, D.D., 1980. Geochemistry of molybdenum in some stream sediments and waters. Geochim. Cosmochim. Acta 44, 447–456.

Katz, B.G., Crandall, C.A., Metz, P.A., McBride, W.S., Berndt, M.P., 2007. Chemical characteristics, water sources and pathways, and age distribution of ground water in the contributing recharge area of a public-supply well near Tampa, Florida, 2002–05. USGS Scientific Investigations Report, pp. 2007–5139 (85 pp).

Katz, B.G., McBride, W.S., Hunt, A.G., Crandall, C.A., Metz, P.A., Eberts, S.M., Berndt, M.P., 2009. Vulnerability of a public supply well in a karstic aquifer to contamination. Ground Water 47 (3), 438–452.

Koterba, M.T., Wilde, F.D., Lapham, W.W., 1995. Groundwater data collection protocols and procedures for the National Water Quality Assessment Program: collection and documentation of water-quality samples and related data. US Geol. Surv. Open-File Report, pp. 95–399.

Lazareva, O., Pichler, T., 2007. Naturally occurring arsenic in the Miocene Hawthorn Group, Southwestern Florida: implication for phosphate mining. Appl. Geochem. 22 (5), 953–973.

Lazareva, O., Druschel, G., Pichler, T., 2015. Understanding arsenic behavior in carbonate aquifers: implications for aquifer storage and recovery (ASR). Appl. Geochem. 52, 57–66.

Lin, T.Y., Hafeznezami, S., Rice, L., Lee, J., Maki, A., Sevilla, T., Stahl, M., Neumann, R., Harvey, C., Suffet, I.H., Badruzzaman, A.B.M., Jay, J.A., 2017. Arsenic oxyanion binding to NOM from dung and aquaculture pond sediments in Bangladesh: importance of site-specific binding constants. Appl. Geochem. 78, 234–240.

Miller, J.A., 1986. Hydrogeologic framework of the Floridan aquifer system in Florida, Georgia, South Carolina and Alabama, U.S. Geol. Surv. Prof. Pap. 1403-B B1–B91.

Nielsen, D.M., Schalla, R., 2006. Design and installation of ground-water monitoring wells. In: Nielsen, D.M. (Ed.), Practical Handbook of Environmental Site Characterization and Ground-water Monitoring. CRC/Taylor & Francis, Boca Raton, FL, pp. 640–805.

Parkhurst, D., Appelo, C., 1999. User's Guide to PHREEQC (Version 2). A Computer Program for Speciation, Batch-reaction, One-dimensional Transport, and Inverse Geochemical Calculations. 1999. U.S. Geological Survey, Reston, VA.

Pichler, T., Mozaffari, A., 2015. Occurrence, distribution and mobility of geogenic molybdenum and arsenic in a limestone aquifer matrix. Appl. Geochem. 63, 623–633.

Pichler, T., Price, R.E., Lazareva, O., Dippold, A., 2011. Determination of arsenic concentration and distribution in the Floridan aquifer system. J. Geochem. Explor. 111 (3), 84–96.

Pichler, T., Renshaw, C.E., Sültenfuß, J., 2017. Geogenic As and Mo groundwater contamination caused by an abundance of domestic supply wells. Appl. Geochem. 77, 68–79.

Planer-Friedrich, B., London, J., McCleskey, R.B., Nordstrom, D.K., Wallschläger, D., 2007. Thioarsenates in geothermal waters of Yellowstone National Park: determination, preservation, and geochemical importance. Environ. Sci. Technol. 41, 5245–5251.

Price, R.E., Pichler, T., 2006. Abundance and mineralogical association of arsenic in the Suwannee limestone (Florida): implications for arsenic release during water–rock interaction. Chem. Geol. 228, 44–56.

Price, R.E., Amend, J., Pichler, T., 2007. Enhanced geochemical gradients in a marine shallow-water hydrothermal system: unusual arsenic speciation in horizontal and vertical pore water profiles. Appl. Geochem. 22, 2595–2605.

Prommer, H., Barry, D.A., Zheng, C., 2003. MODFLOW/MT3DMS based reactive multicomponent transport modeling. Ground Water 41 (2), 247–257.

Reisinger, H.J., Burris, D.R., Hering, J.G., 2005. Remediating subsurface arsenic contamination with monitored natural attenuation. Environ. Sci. Technol. 39 (22), 458a–464a.

Richards, L.A., Magnone, D., van Dongen, B.E., Ballentine, C.J., Polya, D.A., 2015. Use of lithium tracers to quantify drilling fluid contamination for groundwater monitoring in Southeast Asia. Appl. Geochem. 63, 190–202.

Ruda, T., Farrar, J., 2006. Environmental drilling for soil sampling, rock coring, borehole logging, and monitoring well installation. In: Nielsen, D.M. (Ed.), Practical Handbook of Environmental Site Characterization and Ground-water Monitoring. CRC/Taylor & Francis, Boca Raton, FL, pp. 297–346.

Smith, R.M., Martell, A.E., 1976. Critical Stability Constants, Inorganic Complexes. vol. 4. Plenum, New York.

Southwest Florida Water Management District, 2001. The Hydrology and Water Quality of Select Springs in the Southwest Florida Water Management District. Southwest Florida Water Management District, Brooksville, p. 149.

Swedlund, P.J., Webster, J.G., 1999. Adsorption and polymerization of silicic acid on ferrihydrite and its effect on arsenic adsorption. Water Res. 33, 3413–3422.

Tribovillard, N., Riboulleau, A., Lyons, T., Baudin, F., 2004. Enhanced trapping of molybdenum by sulfurized marine organic matter of marine origin in Mesozoic limestones and shales. Chem. Geol. 213 (4), 385–401.

Turner, B.D., Binning, P., Stipp, S.L.S., 2005. Fluoride removal by calcite: evidence for fluorite precipitation and surface adsorption. Environ. Sci. Technol. 39, 9561.

Wallis, I., Prommer, H., Simmons, C.T., Post, V., Stuyfzand, P.J., 2010. Evaluation of conceptual and numerical models for arsenic mobilization and attenuation during managed aquifer recharge. Environ. Sci. Technol. 44 (13), 5035–5041.

Wallis, I., Prommer, H., Pichler, T., Post, V., Norton, S.B., Annable, M.D., Simmons, C.T., 2011. Process-based reactive transport model to quantify arsenic mobility during aquifer storage and recovery of potable water. Environ. Sci. Technol. 45, 6924–6931.

Wang, S., Mulligan, C.N., 2006. Effect of natural organic matter on arsenic release from soils and sediments into groundwater. Environ. Geochem. Health 28 (3), 197–214.

Wichard, T., Mishra, B., Myneni, S.C., Bellenger, J.-P., Kraepiel, A.M.L., 2009. Storage and bioavailability of molybdenum in soils increased by organic matter complexation. Nat. Geosci. 2, 625–629.

Williamson, M.A., Rimstidt, J.D., 1994. The kinetics and electrochemical rate-determining step of aqueous pyrite oxidation. Geochim. Cosmochim. Acta 58 (24), 5443–5454.

Xu, T., White, S.P., Pruessm, K., 2008. Pyrite Oxidation in Saturated and Unsaturated Porous Media Flow: A Comparison of Alternative Mathematical Modeling Approaches. Lawrence Berkeley National Laboratory. Open Access Publication.